

Published in final edited form as:

Curr Biol. 2011 April 12; 21(7): 598–605. doi:10.1016/j.cub.2011.02.049.

Amphiastral Mitotic Spindle Assembly in Vertebrate Cells Lacking Centrosomes

Jessica E. Hornick^{1,*}, Christopher C. Mader^{2,3,*}, Emily K. Tribble^{4,*}, Cydney C. Bagne⁵, Kevin T. Vaughan⁶, Sidney L. Shaw⁷, and Edward H. Hinchcliffe^{5,†}

¹ Department of Obstetrics and Gynecology, and the Robert H. Lurie Cancer Center, Northwestern University School of Medicine, Chicago, IL 60611 USA

² Department of Cell Biology, Yale University, New Haven, CT 06510 USA

³ Department of Chemistry, Northwestern University, Evanston, IL 60208 USA

⁴ Department of Cell and Developmental Biology, University of North Carolina, School of Medicine, Chapel Hill, NC 27599 USA

⁵ Cellular Dynamics Section, The Hormel Institute, University of Minnesota Austin, MN 55912 USA

⁶ Department of Biological Sciences, and the Notre Dame Integrated Imaging Facility, University of Notre Dame, Notre Dame, IN 46556 USA

⁷ Departments of Biology and Physics, Indiana University, Bloomington, IN 47405 USA

Summary

The role of centrosomes/centrioles during mitotic spindle assembly in vertebrates remains controversial. In cell-free extracts and experimentally derived acentrosomal cells, randomly oriented microtubules (MTs) self-organize around mitotic chromosomes and assemble anastral spindles [1,2,3]. However, vertebrate somatic cells normally assemble a connected pair of polarized, astral MT arrays – termed an *amphiaster* (“a star on both sides” [4]) – that is formed by the splitting and separation of the microtubule-organizing center (MTOC) well before nuclear envelope breakdown (NEB) [5]. Whether amphiaster formation requires splitting of duplicated centrosomes is not known. We found that when centrosomes were removed from living vertebrate cells early in their cell cycle, an acentriolar MTOC re-assembled, and prior to NEB, a functional amphiastral spindle formed. Cytoplasmic dynein, dynactin, and pericentrin are all recruited to the interphase aMTOC, and the activity of kinesin-5 is needed for amphiaster formation. Mitosis proceeded on time and these karyoplasts divided in two. However, ~35% of aMTOCs failed to split/separate before NEB, and these entered mitosis with persistent monastral spindles. The chromatin-mediated RAN-GTP pathway could not restore bipolarity to monastral spindles, and these cells exited mitosis as single daughters. Our data reveal the novel finding that MTOC separation and amphiaster formation does not absolutely require the centrosome, but in its absence, the fidelity of bipolar spindle assembly is highly compromised.

[†]Correspondence should be addressed to EHH, ehinchcliffe@hi.umn.edu.

*These authors contributed equally to this work

Publisher's Disclaimer: This is a PDF file of an unedited manuscript that has been accepted for publication. As a service to our customers we are providing this early version of the manuscript. The manuscript will undergo copyediting, typesetting, and review of the resulting proof before it is published in its final citable form. Please note that during the production process errors may be discovered which could affect the content, and all legal disclaimers that apply to the journal pertain.

Keywords

Amphiaster; centrosome; centriole; monaster; microtubule; mitosis; spindle

Results and discussion

Unlike flowering plant cells, animal somatic cells do not completely disassemble their microtubule (MT) network at the G₂/M transition, thus retaining the burden of managing a polarized, radial MT array throughout the transition into mitosis [6,7]. The single MT focus splits into a connected pair of astral arrays, historically known as an amphiaster [4]. Amphiaster formation has traditionally been ascribed to the splitting and separation of the duplicated centrosomes, which precedes bipolar spindle assembly [5,8,9,10]. However, whether vertebrate somatic cells actually require the presence and/or duplication of centrosomes in order to split their MT array during spindle assembly is not known. To test this, we used microsurgery [11] to remove the centrosome from monkey (BSC-1) cells constitutively expressing α tubulin-GFP [12], and followed their behavior using live imaging.

For microsurgery, the microneedle was brought down between the centrosome and the nucleus (Figure 1), and the cell separated into two fragments: a nuclear-containing cell lacking a centrosome (termed the karyoplast or KP) and an enucleate fragment containing the centrosome (termed the cytoplasm, or CP). Often the CP was removed using the microneedle so that it did not obscure the events in the KP. We selected cells with a distinct “tri-corners” morphology to ensure that the centrosome was located in the presumptive CP, regardless of whether it had duplicated (see Figure S1C). The position of the KP on the coverslip was marked with a diamond scribe mounted in the nosepiece of the microscope, and living KPs were examined using the time-lapse microscopy [11]. As a control for the loss of cytoplasm, equivalent masses of cytoplasm were removed, but the centrosomes were left in the cell. In 9/9 cases, these control-cut cells formed bipolar spindles (Figure S1, also see [11]), and proceeded through mitosis within the range of normal mitotic timing (Figure 2C).

We first asked whether KPs could reform an *acentriolar MTOC* (aMTOC; [13]). Ten KPs were examined, beginning one hr after microsurgery, a time when the KP had flattened. In each case, the organization of the MT network was initially disrupted, and then became re-organized into a single radial array, with its focus near the nucleus (Figure 1B, f, arrow). The reformation of the aMTOC in the KP occurred over a period of ~6 hrs following microsurgery, a timeframe similar to that observed for MT self-centering in enucleate fragments of melanophores [14,15]. The centrioles in BSC-1 KPs do not reform during interphase, as judged by same cell live-imaging and immunolabeling with anti-centrin 2 (N = 3; Figure 1C).

Spindle assembly in acentriolar karyoplasts

Next, live-cell imaging was used to examine the mode of mitotic spindle assembly in KPs (Figure 2). KPs were generated by microsurgery and followed using differential interference contrast (DIC) optics, in order to minimize potential photodamage to the cells [16]. When the KPs were judged to be near the G₂/M transition (determined by a change in the morphology of the nucleolus) the microscope was switched from DIC to confocal fluorescence optics, and spindle assembly was imaged (Figure 2). In all cases a single MT focus was observed prior to NEB (Figure 2A, B). However, spindle assembly in KPs occurred in two distinct modes: (I) the formation of an amphiaster prior to NEB, followed

by the formation of a bipolar spindle, and (II) formation of a monaster, followed by monopolar spindle assembly.

Of the 76 KPs examined, 46 (61%) underwent splitting of the aMTOC into an amphiastral array, which remained closely apposed to the nuclear envelope (Figure 2A, f–h, insets). These amphiastrs then assembled into bipolar spindles (Figure 2, i–l), and progressed through mitosis – measured as the time from NEB to anaphase onset (avg. = 65 min, range 30 – 125 min). This compares with the mitotic timing for control cells (avg. = 46 min, range 24 – 99 min; Figure 2C).

In contrast, the single MT array failed to split or separate prior to NEB in 26/76 KPs (34%) (Figure 2B, e–h). Instead, the MTs remained as a monastral array, and these KPs assembled monopolar spindles. The time from NEB to anaphase onset in KPs with monastral spindles (avg. = 285 min, range 180 – 480 min; Figure 2C) was longer than that of amphiastral KPs or control cells. Anaphase onset in monastral spindles was easily judged by the polarization of the karyoplast and the lengthening of the monopolar spindle [see ref. 17]. Interestingly, when monopolar KPs eventually exited mitosis, they formed multiple cytokinetic furrows, which eventually retracted, resulting in a single polyploid daughter (data not shown). We also note that the MT network in KPs destined to form monopolar spindles was not noticeably diminished (data not shown). MTs in these KPs were observed extending to the cell cortex, suggesting that this is not the underlying cause for failure to form a bipolar spindle.

Examination of a karyoplast during amphiastr formation revealed that the asters lack centrioles, but do contain reduced γ -tubulin (Figure 2D). Post-mitotic karyoplasts that built an amphiastr and divided into two (N=2; Figure 2) or built a monopolar and failed cytokinesis (N=2; Figure S1A) also lacked centrioles. In 24/26 cases where we examined KPs for centrioles using same-cell live and immunofluorescence imaging, we found that the centrioles had been removed. Previous work had demonstrated that post-mitotic BSC-1 KPs lack centrioles, as judged by serial section electron microscopy [11]. However, in other cell types, notably CHO, HeLa, and RPE-1 cells, a variable numbers of centrioles can reform *de novo* during S-phase [16, 18, 19]. Because we cannot distinguish between G₁ cells (with a pair of centrioles) and G₂ cells (with a duplicated pair centrioles; see Figure S1), it is formally possible that some KPs could have reformed centrioles *de novo* during S-phase. Regardless, Figure 2D demonstrates that amphiastr splitting and separation can occur with the bipolar cue provided by centrioles.

The acentriolar MTOC and MT organization in karyoplasts

Given that amphiastr formation in acentrosomal cells is error prone, we examined potential differences between KPs that either could or could not split their asters. Centrioles themselves nucleate particular sub-classes of MTs, and the remaining MTs are nucleated by the PCM surrounding the centrioles [20]. However, cohesion of the MTOC as a whole is mediated, at least in part, by cytoplasmic dynein and its co-factor dynactin [21,22,23]. Dynein also plays a key role in separating the duplicated centrosomes during normal amphiastr formation [24]. In addition, the structural protein pericentrin, along with γ -tubulin is transported to the MTOC by dynein, where they are involved in maintaining MT organization [25,26]. Together, dynein, dynactin, and pericentrin could potentially play a role in re-establishing the MTOC following removal of the centrosome by microsurgery.

Using same-cell live and immunofluorescence microscopy of KPs immediately after microsurgery, we examined the extent to which pericentrin, dynein and dynactin re-localized the aMTOC as it re-assembled. The distribution of these MTOC components in KPs was compared to that in the adjacent centrosome-containing CPs (Figure 3, panels marked with

an asterisk). We examined the distribution of these proteins in KPs at times both before ($T = 1.5$ hrs) and after ($T = 6$ hrs) the reformation of the radial MT array. For each condition, we examined three separate karyoplasts. These proteins all localize to the MTOC in control BSC-1 cells (Figure S2).

At $T = 1.5$ hrs post-microsurgery, the localization of pericentrin, dynein and dynactin to the MTOC was lost along with the MT array (Figure 3A–C). As the MT network reformed ~6 hrs post microsurgery, pericentrin, dynein, and dynactin all became re-focused to the nascent aMTOC (Figure 3). Note that the centrosomes residing in the anucleate CPs retained their focus of pericentrin dynein, and dynactin (Figure 3A–C, asterisks).

Another cellular structure that is assembled in the vicinity of the MTOC is the Golgi network, which in addition to mediating protein sorting and vesicle transport, also serves to organize non-centrosomal MTs, and is itself dependant on dynein-mediated motility [27,28]. As a measure of MTOC reformation, the organization of the Golgi was examined in KPs following microsurgery (Figure 3B). At $T = 1.5$ hrs following microsurgery the Golgi was disrupted in the KP (Figure 3B, c'). At $T = 6\frac{1}{2}$ hrs the Golgi had reformed to approximately control levels (Figure 2B, f'). Thus, as the radial acentriolar MT array re-forms in KPs, pericentrin, dynein, dynactin, and a morphologically normal Golgi network associate with the aMTOC.

Organization of the acentriolar MTOC in post-mitotic karyoplasts

We next examined the organization of the aMTOC in post-mitotic KPs. Same-cell live and immunofluorescence microscopy of KPs that divided into two revealed that these KPs contained a robust focus of pericentrin at the aMTOC (Figure 4A, panel f'' insets, $N=5$), and dynein ($N = 3$, data not shown). Note the centrosomal focus of pericentrin seen in the lone cytoplasm remaining on the coverslip (Figure 4A, f'' lower inset). We also found γ -tubulin, albeit in reduced amounts, in the asters separating at the onset of mitosis in karyoplasts (Figure 2). Thus, in post-mitotic KPs that underwent bipolar division, the aMTOCs each contained a focus of pericentrin, dynein, and γ -tubulin, indicating reformation of partial PCM in the absence of centrioles.

When KPs that failed cytokinesis were examined, we found that these lacked a distinct focus of pericentrin ($N = 3$, Figure 4B), or dynein ($N = 3$, data not shown). Monopolar KPs also lack a post-mitotic focus of γ -tubulin (Figure S1). The obvious differences in the aMTOC composition between KPs that underwent bipolar vs. monopolar division suggest that the failure to form an amphiaster and a bipolar spindle could be caused by an insufficient recruitment of MTOC components, such as pericentrin, dynein or γ -tubulin to the MT minus ends as they coalesced following microsurgery.

Finally, we examined the role of kinesin 5 on the splitting and separation of the aMTOC. Kinesin-5 is a MT motor involved in driving centrosome-containing spindle poles apart during spindle assembly [29,30]. KPs were generated by microsurgery, and after they had healed and flattened out, $100 \mu\text{M}$ monastrol was added to inhibit kinesin 5 activity. In 10/10 KPs treated with monastrol, all failed bipolar spindle formation, were delayed in mitosis, and eventually failed cytokinesis (Figure S3). In 35/35 control cells treated with monastrol, all were delayed in mitosis, and all exited mitosis as single daughter cells (Figure S3). Thus, the separation of the aMTOC into an amphiaster appears to be dependant on kinesin-5 motility.

Conclusions

Our results reveal several novel aspects of the role of the centrosome during mitotic spindle assembly in vertebrate somatic cells. There has been a long-standing notion that the separation of duplicated centrosomes drives bipolar spindle assembly in these types of cells [8,9,31]. As the asters separate, the dynamic MT plus-ends interact, pushing the asters apart through the action of their associated motor proteins [30,32]. The extent of spindle pole separation prior to NEB varies, and also appears dependent on MT interactions with the cell cortex [33,34,35], and on the action of the kinetochore MTs [36].

We find that in the absence of a centrosome and centrioles, karyoplasts always reform a single perinuclear MT array that is capable of disjunction and separation to form two distinct spindle poles. Importantly, this splitting occurs in a strict one-to-two fashion, and prior to NEB – well before MTs could interact with the chromosomes and Ran-GTP gradient that drives bipolar spindle assembly in other acentrosomal systems [37]. While these MTOCs lack centrioles, they do re-focus dynein, dynactin pericentrin and γ -tubulin to varying degrees, and post-mitotic KPs that have undergone bipolar division have a focus of pericentrin dynein and γ -tubulin at their MTOC (Figure 4).

However, in contrast to other acentrosomal systems, which form bipolar spindles in essentially all cases [1,2,3], the fidelity of bipolar spindle assembly in KPs is compromised. 34% of the aMTOCs failed to separate prior to NEB, and monasters exerted a dominant influence over spindle assembly. Examination of post-mitotic KPs that form monasters and fail cytokinesis revealed that these lack appreciable amounts of PCM at the aMTOC.

Why do some karyoplasts form amphiasters and bipolar spindles, while others do not? It is possible that post-mitotic KPs that underwent monastral division lacked sufficient pericentrin, dynein or γ -tubulin at their aMTOC to allow splitting of the MT focus (see Figures 2 and 4). This suggests that normally some component of the centrosome – perhaps the centrioles – is responsible for the recruitment of PCM in quantities sufficient for the cohesion and the eventual splitting of the MTOC. In the absence of centrosomes, the recruitment of PCM cannot be assured, and the incidence of monopolar spindle assembly increases to catastrophic levels. It also remains a possibility that residual Golgi, left after the microsurgery, could be responsible for recruiting sufficient PCM to the aMTOC to allow for amphiaster formation. Whether the centrosome and Golgi act in a coordinated fashion or are redundant mechanisms for PCM assembly and re-focusing of the MT network remains to be determined [38].

Our finding that monastral spindles persist throughout mitosis in acentrosomal cells is also intriguing because it is known that centrosome separation can occur well after NEB and mitotic onset [9,10]. BSC-1 cells treated with monastrol form monopolar spindles, yet the centrosomes separate and form a bipolar spindle when the drug is washed out [29,30]. We find spontaneous monopoles in control BSC-1 cells that eventually resolved into bipolar spindles, and divided into two (Figure S3). However, in karyoplasts that lack centrosomes, monastral spindles form that cannot be corrected for, with disastrous consequences for cell division.

In conclusion, our results reveal that centrosomes are necessary in order to ensure that bipolar spindle assembly occurs with high fidelity. While centrioles appear to be dispensable for the organization of the PCM, and for the splitting of the resulting aMTOC into an amphiaster, we show that in their absence, defects in spindle assembly arise. Karyoplasts lacking centrioles have defects in their ability to reform their PCM and the necessary splitting/separation of the aMTOC does not always occur. This results in the generation of

monopolar spindles that cannot be compensated for by the chromatin-mediated spindle assembly pathway.

Experimental Procedures

Unless otherwise noted all reagents were obtained from Sigma Chemical Co. (St. Louis, MO).

Cell Culture and treatment

BSC-1 cells (African Green Monkey kidney cells; ATCC, Manassas, VA) were cultured in DMEM containing 10% FBS (Gibco, Grand Island, NY) and 1 mg/ml pen-strep (Sigma-Aldrich, St. Louis, MO) in 10% CO₂. These were used as is, or transfected with EGFP- α tubulin (Clontech, Mountain View, CA) using Fugene 6 (Roche Applied Science, Indianapolis, IN), and selected with G418 (2 mg/ml). Clones were identified as described [12].

100 μ M Monastrol (CalBiochem, La Jolla, CA) was added 6 hrs after microsurgery.

Microsurgery, live-cell microscopy, and fluorescence microscopy

For microsurgery, BSC-1 EGFP- α tubulin cells were plated onto bio-cleaned glass coverslips in Imaging Media (DMEM w/o phenol red, containing 12 mM HEPES, pH 7.2, 10% fetal bovine serum) and assembled onto aluminum support slides [11,39]. Microneedles were pulled using a Kopf vertical pipet puller (Kopf, CA) and the final needle geometry was shaped using a microforge deFonbrune (TPI, St. Louis, MO). Microsurgery was performed with a Burleigh MIS-5000 piezo-electric micromanipulator attached to a pre-warmed Leica DM IRB2 inverted microscope (Leica Microsystems, Bannockburn, IL) equipped with phase contrast optics and a rotating stage. Karyoplast position on the coverslip was marked with a diamond scribe.

Time-lapse images were captured using a Leica DM RXA2 microscope stand using a 40 \times /0.7 NA objective, and enclosed in a custom-made Plexiglas box maintained at 37 $^{\circ}$ C. Live-cell fluorescence images were also captured with a Yokogawa CSU-10 spinning disk confocal head, as modified by McBain Systems (Simi Valley, CA), using a Leica 63 \times /1.3 NA glycerol-immersion objective, a Coherent 200 mW 488 nm laser (Coherent Inc. Santa Clara, CA), and a Hamamatsu 9100 back-thinned EM-CCD camera.

Cells on coverslips were fixed in -20 $^{\circ}$ C methanol. Cells were labeled with anti-centrin 2 (1:1000; mouse monoclonal; gift of Dr. Jeff Salisbury, Mayo Medical School), anti- γ -tubulin (1:1000, rabbit polyclonal, Sigma), anti-dynein IC (1:300 [ref. 40]), anti-p150 dynactin (1:300 [ref. 41]), anti-pericentrin (1:2000, Abcam, Cambridge, MA), or anti-GM-130/Golgi (1:1000, Santa Cruz Biologicals). The 2 $^{\circ}$ antibodies were the species appropriate conjugates with Alexa-488, Alexa-594, or Alexa-660 at a 1:1000 dilution (Invitrogen, Carlsbad, CA). Cells were counter stained with DAPI (Sigma) and mounted in 10% PBS, 90% glycerol. Fixed cells were imaged with a 63X 1.4 NA oil objective on a Leica DM RXA2 microscope using a Hamamatsu ORCA-ER CCD camera; 0.2 μ m Z-stacks were compiled as maximum projections. Images were acquired with Simple PCI (Compix, Sewickley, PA) or Slidebook software (Intelligent Imaging Innovations, Denver Colorado). Some images were subjected to 2-D blind deconvolution (Simple PCI, Compix). Figures were assembled using Photoshop 6.0 (Adobe, San Jose, CA).

Supplementary Material

Refer to Web version on PubMed Central for supplementary material.

Acknowledgments

We thank Dr. Jeff Salisbury for his generous gift of centrin 2 antibody, Drs. JoEllen Welsh and Holly Goodson for comments during the course of this work, Mr. Rick Miller for assistance in the initial fabrication of the microneedles, and Mr. Kul Karanjeet for technical assistance. JEH was supported by training grants from the NIH (T32 GM075762 and T32 CA080621). CCM was supported by a graduate research fellowship from the National Science Foundation. SLS was funded by a research grant from the National Science Foundation (NSF 0920555). KTV and EHH were supported by Research Scholar grants from the American Cancer Society. EHH was supported by funds from the Hormel Institute, the Lyle Area Cancer Auction, and the Minnesota 5th District Eagles Cancer Telethon. This work was supported by research grants from NIGMS to KTV (GM060560) and EHH (GM072754).

References

1. Heald R, Tournebise R, Blank T, Sandaltzopoulos R, Becker P, Hyman A, Karsenti E. Self-organization of microtubules into bipolar spindles around artificial chromosomes in *Xenopus* egg extracts. *Nature*. 1996; 382:420–425. [PubMed: 8684481]
2. Khodjakov A, Cole RW, Oakley BR, Rieder CL. Centrosome-independent mitotic spindle formation in vertebrates. *Curr Biol*. 2000; 10:59–67. [PubMed: 10662665]
3. Mahoney NM, Goshima G, Douglass A, Vale RD. Making microtubules and mitotic spindles in cells without functional centrosomes. *Curr Biol*. 2006; 16:564–69. [PubMed: 16546079]
4. Taylor EW. Dynamics of spindle formation and its inhibition by chemicals. *J Biophys Biochem Cytol*. 1959; 6:193–198.
5. Walczak CE, Heald R. Mechanisms of mitotic spindle assembly and function. *Int Rev Cytol*. 2008; 265:111–158. [PubMed: 18275887]
6. Lloyd C, Chan J. Not so divided: the common basis of plant and animal cell division. *Nat Rev Mol Cell Biol*. 2006; 7:147–152. [PubMed: 16493420]
7. Bannigan A, Lizotte-Waniewski M, Riley M, Baskin TI. Emerging molecular mechanisms that power and regulate the anastral mitotic spindle of flowering plants. *Cell Motil Cyto*. 2008; 65:1–11.
8. Mazia D. The chromosome cycle and the centrosome cycle in the mitotic cycle. *Int Rev Cytol*. 1987; 100:49–92. [PubMed: 3549609]
9. Rosenblatt J. Spindle assembly: asters part their separate ways. *Nat Cell Biol*. 2005; 7:219–222. [PubMed: 15738974]
10. Hinchcliffe EH, Sluder G. “It takes two to tango”: understanding how centrosome duplication is regulated throughout the cell cycle. *Genes Dev*. 2001; 15:1167–1181. [PubMed: 11358861]
11. Hinchcliffe EH, Miller FJ, Cham M, Khodjakov A, Sluder G. Requirement of a centrosomal activity for cell cycle progression through G₁ into S phase. *Science*. 2001; 291:1547–1550. [PubMed: 11222860]
12. Hornick JE, Bader J, Trimble K, Tribble EK, Breunig JS, Halpin ES, Vaughan KT, Hinchcliffe EH. Live-cell analysis of mitotic spindle formation in taxol-treated cells. *Cell Motil Cyto*. 2008; 65:1–19.
13. Moutinho-Pereira S, Debec A, Maiato H. Microtubule cytoskeleton remodeling by acentriolar microtubule-organizing centers at the entry and exit from mitosis in *Drosophila* somatic cells. *Mol Biol Cell*. 2009; 20:2796–2808. [PubMed: 19369414]
14. McNiven MA, Porter KR. Organization of microtubules in centrosome-free cytoplasm. *J Cell Biol*. 1988; 106:1593–1605. [PubMed: 3286659]
15. Rodionov VI, Borisy GG. Self-centering activity of cytoplasm. *Nature*. 1997; 386:170–173. [PubMed: 9062188]
16. Uetake Y, Lončarek J, Nordberg JJ, English CN, La Terra S, Khodjakov A, Sluder G. Cell cycle progression and *de novo* centriole assembly after centrosomal removal in untransformed human cells. *J Cell Biol*. 2007; 176:173–182. [PubMed: 17227892]
17. Hu CK, Coughlin M, Field CM, Mitchison TJ. Cell polarization during monopolar cytokinesis. *J Cell Biol*. 2008; 181:195–202. [PubMed: 18411311]
18. Khodjakov A, Rieder CL, Sluder G, Cassels G, Sibon O, Wang CL. *De novo* formation of centrosomes in vertebrate cells arrested during S phase. *J Cell Biol*. 2002; 158:1171–1181. [PubMed: 12356862]

19. LaTerra S, English CN, Hergert P, McEwen BF, Sluder G, Khodjakov A. The de novo centriole assembly pathway in HeLa cells: cell cycle progression and centriole assembly/maturation. *J Cell Biol.* 2005; 168:713–722. [PubMed: 15738265]
20. Bornens M. Centrosome composition and microtubule anchoring mechanisms. *Curr Opin Cell Biol.* 2002; 14:25–34. [PubMed: 11792541]
21. Vaisberg EA, Koonce MP, McIntosh JR. Cytoplasmic dynein plays a role in mammalian mitotic spindle formation. *J Cell Biol.* 1993; 123:849–858. [PubMed: 8227145]
22. Robinson JT, Wojcik EJ, Sanders MA, McGrail M, Hays TS. Cytoplasmic dynein is required for the nuclear attachment and migration of centrosomes during mitosis in *Drosophila*. *J Cell Biol.* 1999; 146:597–608. [PubMed: 10444068]
23. Quintyne NJ, Gill SR, Eckley D, Crego C, Compton DA, Schroer TA. Dynactin is required for microtubule anchoring at centrosomes. *J Cell Biol.* 1999; 147:321–334. [PubMed: 10525538]
24. Tanenbaum ME, Macůrek L, Galjart N, Medema RH. Dynein, Lis1 and CLIP-170 counteract Eg-5-dependent centrosome separation during bipolar spindle assembly. *EMBO J.* 2008; 27:3235–3245. [PubMed: 19020519]
25. Purohit A, Tynan SH, Vallee R, Doxsey SJ. Direct interaction of pericentrin with cytoplasmic dynein light intermediate chain contributes to mitotic spindle organization. *J Cell Biol.* 1999; 147:481–491. [PubMed: 10545494]
26. Young A, Dichtenberg JB, Purohit A, Tuft R, Doxsey SJ. Cytoplasmic dynein-mediated assembly of pericentrin and gamma tubulin onto centrosomes. *Mol Biol Cell.* 2000; 11:2047–2056. [PubMed: 10848628]
27. Vaughan KT. Microtubule plus ends, motors, and traffic of Golgi membranes. *Biochem Biophys Acta.* 2005; 1744:316–24. [PubMed: 15950296]
28. Efimov A, Kharitonov AA, Efimova N, Lončarek J, Miller PM, Andreyeva N, Gleeson P, Galjart N, Maia ARR, McLeod IX, Yates JR III, Maiato H, Khodjakov A, Akhmanova A, Kaverina I. Asymmetric CLASP-dependent nucleation of non-centrosomal microtubules at the trans-Golgi network. *Dev Cell.* 2007; 12:917–930. [PubMed: 17543864]
29. Kapoor TM, Mayer TU, Coughlin ML, Mitchison TJ. Probing spindle assembly mechanisms with monastrol, a small molecule inhibitor of the mitotic kinesin, Eg5. *J Cell Biol.* 2000; 150:975–988. [PubMed: 10973989]
30. Ferenz NP, Paul R, Fagerstrom C, Mogilner A, Wadsworth P. Dynein antagonizes Eg5 by crosslinking and sliding antiparallel microtubules. *Curr Biol.* 2009; 19:1833–38. [PubMed: 19836236]
31. Lim H, Zhang T, Surana U. Regulation of centrosome separation in yeast and vertebrates: common threads. *Trends Cell Biol.* 2009; 19:325–333. [PubMed: 19576775]
32. Sharp DJ, Rogers GC, Scholey JM. Microtubule motors in mitosis. *Nature.* 2000; 407:41–7. [PubMed: 10993066]
33. Waters JC, Cole RW, Rieder CL. The force-producing mechanism for centrosome separation during spindle formation in vertebrates is intrinsic to each aster. *J Cell Biol.* 1993; 122:361–372. [PubMed: 8320259]
34. Rosenblatt J, Cramer LP, Baum B, McGee KM. Myosin II-dependant cortical movement is required for centrosome separation and positioning during mitotic spindle assembly. *Cell.* 2004; 117:361–372. [PubMed: 15109496]
35. Cao J, Crest J, Fasulo B, Sullivan W. Cortical actin dynamics facilitate early-stage centrosome separation. *Curr Biol.* 2010; 20:770–776.
36. Toso A, Winter JR, Garrod AJ, Amaro AC, Meraldi P, McAinsh AD. Kinetochore-generated pushing forces separate centrosomes during bipolar spindle assembly. *J Cell Biol.* 2009; 184:365–372. [PubMed: 19204145]
37. Kaláb P, Pralle A, Isacoff EY, Heald R, Weis K. Analysis of a RanGTP-regulated gradient in mitotic somatic cells. *Nature.* 2006; 440:697–701. [PubMed: 16572176]
38. Sütterlin C, Colanzi A. The Golgi and the centrosome: building a functional partnership. *J Cell Biol.* 2010; 188:621–628. [PubMed: 20212314]

39. Durcan T, Halpin ES, Rao T, Collins N, Tribble EK, Hornick JE, Hinchcliffe EH. Tektin 2 is required for central spindle microtubule organization and the completion of cytokinesis. *J Cell Biol.* 2008; 181:595–603. [PubMed: 18474621]
40. Whyte J, Bader JR, Tauhata SBF, Raycroft M, Hornick J, Pfister KK, Lane WS, Chan GK, Hinchcliffe EH, Vaughan PS, Vaughan KT. Phosphorylation regulates targeting of cytoplasmic dynein to kinetochores during mitosis. *J Cell Biol.* 2008; 183:819–834. [PubMed: 19029334]
41. Vaughan PS, Miura P, Henderson M, Byrne B, Vaughan KT. A role for regulated binding of p150^{Glued} to microtubule plus ends in organelle transport. *J Cell Biol.* 2002; 158:305–319. [PubMed: 12119357]

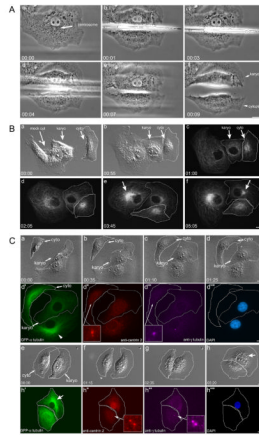


Figure 1. Microsurgical removal of the centrosome from BSC-1 cells

Aa. The centrosome is identified by a mass of granules adjacent to the nucleus (arrow). **Ab–Ae.** The needle is brought down between the nucleus and the centrosome. **Af.** The nuclear containing karyoplast (Karyo or KP) is completely separated from the centrosome containing cytoplast (cyto or CP). **B. MT network reformation in the KP/CP pair. Ba–c.** Two cells following microsurgery. The first is a mock-cut, where the centrosome is displaced from the nucleus by the needle, but the CP is not severed from the KP. The second cell is cut by the needle, resulting in a KP/CP pair. The KP is surrounded by a white outline. **Bc.** Fluorescence imaging: the mock-cut cell and the KP both lack a perinuclear MT focus, whereas the CP has a radial MT array. **Bd–bf.** The radial MTs reforms in the mock-cut cell (arrow in **e**) and KP (arrow in **Bf**). **C. aMTOC formation in the karyoplast. Ca–Cd.** The KP/CP flatten out over the first 1½ hours. **Cd'–Cd'''.** Same cell immunolabeling of **d**. The MTs in the KP (**d'**) do not have a central focus; the control cell does (arrowhead). The centrin-2 positive centrioles (**Cd''**) and γ -tubulin positive pericentriolar material (**Cd'''**) are in the CP. **Ce–Ch.** The KP/CP pair ~ 5 hrs after microsurgery **Ch'–Ch'''.** Same cell immunofluorescence of **Ch**. The aMTOC has reformed (arrow in **Ch'**). The KP lacks centrioles and PCM; these reside in the CP. Time = Hrs:min. Bars = 10 μ m.

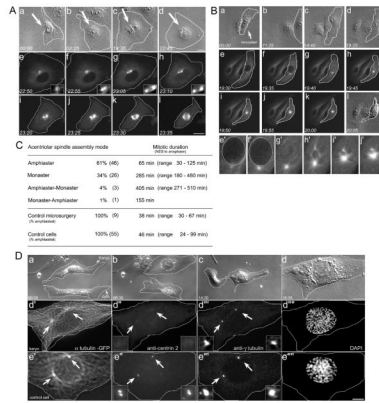


Figure 2. Mitotic spindle assembly in KPs

A. Amphiastal bipolar spindle assembly. **Aa–Ad.** Microsurgery generates a KP (arrow). The CP was removed. **Ae–Ai.** Fluorescence imaging: there is a single MT focus (insets, **Ae–Ah**) that undergoes splitting and amphiaster formation prior to NEB. At NEB (**Ah**) there are two distinct MT foci, which form a bipolar spindle (**Ai–Al**). **B.** Monastral spindle assembly. **Ba–Bd.** Microsurgery forms a KP, (arrow), the CP was removed. **Be–Bk.** Fluorescence imaging: the single MT focus has not split at NEB. Upon entry into mitosis, the MTs are drawn into the monastral array. **Be'–Bj'.** High mag view of monaster during spindle assembly. The nuclear region is outlined. **C.** Mode of spindle assembly in karyoplasts. Control microsurgery represents the removal of equal volumes of cytoplasm, without removal of the centrosome. **D.** Centrioles do not reform in the interphase karyoplasts. **Da–d.** Microsurgery used to remove the centrosome, and the KP/CP pair followed by time-lapse microscopy. When the KP was judged to be entering mitosis, the coverslip was removed from the chamber and fixed. **Dd'–d'''.** The KP fixed just as it entered prophase. There are two distinct MT asters, fixed in the process of separating (arrows). These asters lack centrioles (**Dd''** arrows and insets) but have assembled a somewhat diminished PCM (**Dd'''** arrows and insets). Note the chromosomes are condensed (**Dd'''**). **De'–e'''.** Control cell in prophase, showing separated asters (**De'**, arrows) containing divided pairs of centrioles (**De''**, arrows and insets), and robust arrays of PCM (**De'''**, arrows and insets). Time = Hrs:min. Bars = 10 μ m. Also see Figure S2.

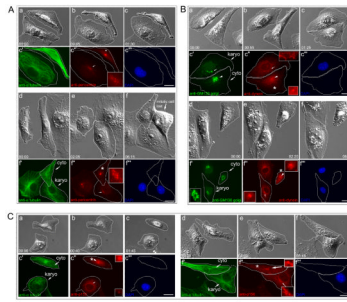


Figure 3. Re-formation of the aMTOC following microsurgery

A. Pericentrin. Aa–Ac. karyo/cyto pair 1½ hrs after microsurgery. The control cell entering mitosis in **Af** is lost following fixation. **Ac'–Ac'''**. Same cell immunofluorescence of **Ac**. The MT network has not reformed, and there is a faint, diffuse cloud of pericentrin adjacent to the nuclear envelope in the KP (**Ac''**, arrow). The centrosomal focus of pericentrin is in the CP (* in **Ac''**). **Ad–Af'''**. After 6 hrs, the aMTOC has reformed with a single focus of pericentrin adjacent to the nuclear envelope (**Af''**, arrow and inset). **B. Cytoplasmic dynein and Golgi apparatus. Ba–Bc'''**. 1½ hrs after microsurgery, the centrosome and bulk of the Golgi are found in the CP (arrowheads in **Bc'–Bc''**). There is little Golgi network in the KP (arrow, **Bc'**), and the KP lacks a focus of cytoplasmic dynein (arrow in **Bc''**, and inset). **Bd–Bf'''**. After 6½ hrs, there is a radial, perinuclear Golgi array (**Bf'**, inset) surrounding a single perinuclear focus of cytoplasmic dynein (**Bf''**, arrow and lower inset). The centrosome is in the CP (**Bf''**, arrowhead and upper inset). **C. Ca–Cc'''**. Dynactin. After 1½ hrs the centrosomal focus of dynactin is located in the CP (**c''**, arrowhead and upper inset), and is lost from the KP (**Cc''**, arrow and lower inset). **Cd–Cf'''**. After ~6 hrs, the aMTOC reforms in the KP. The centrosome is in the CP (**Cf''**, arrowhead and upper inset). There is a perinuclear cloud of dynactin (**Cf''**, arrow and lower inset) co-incident with the MT focus in the KP (**Cf'**, arrow). Time = Hrs:min. Bars = 10µm. Also see Figure S2.

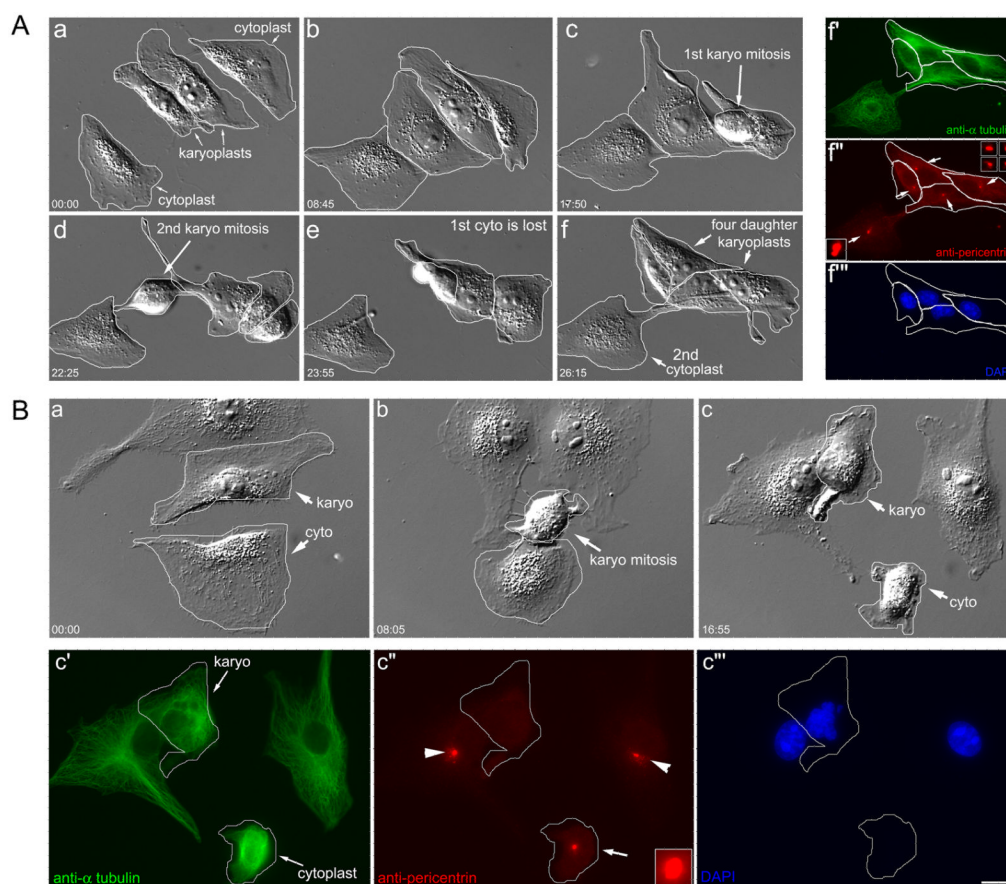


Figure 4. aMTOC reformation in karyoplasts

A. Karyoplasts divide and contain a post-mitotic focus of pericentrin. **Aa–f.** Two KPs proceed through mitosis yielding four daughters. The CP in the top right lyses prior to fixation. **Af'–f'''.** Same-cell immunofluorescence. The four daughter karyoplasts all contain a focus of pericentrin (arrows and insets) comparable to the centrosome in the remaining CP (arrow and inset, lower left). **B.** KP that undergoes a monopolar division lacks a post-mitotic focus of pericentrin. **Ba–c.** KP/CP pair (outline); the KP enters mitosis and exits as a single daughter (**b**). **Bc'–c''.** Same-cell immunofluorescence. The post-mitotic KP (outline) has disorganized MTs and lacks a focus of pericentrin (**Bc''**). The centrosomal pericentrin focus is visible in the CP (arrow), as are the centrosomes in the two adjacent control cells (**Bc''**: arrowheads). DIC and fluorescence optics. Hrs:min. Bar = 10 μ m. Also see Figure S3.